frontiers | Frontiers in Energy Research

TYPE Original Research
PUBLISHED 24 October 2023
DOI 10.3389/fenrg.2023.1291552

OPEN ACCESS

EDITED BY
Rashid Mehmood,
King Abdulaziz University, Saudi Arabia

REVIEWED BY
Zhixuan Gao,
China Electric Power Research Institute (CEPRI), China
Zecheng Li,
State Grid Ningxia Electric Power Research Institute, China
Peng Chen,
Huairou Laboratory, China

*CORRESPONDENCE
Zhengzhong Gao,
skdgzz@163.com

RECEIVED 09 September 2023
ACCEPTED 09 October 2023
PUBLISHED 24 October 2023

CITATION
Feng C, Ye P, Gao Z, Jiang H, Zang X and Zhang X (2023), A novel distributing–collecting on-line insulation monitoring system and line selection technology for the DC supply system. *Front. Energy Res.* 11:1291552. doi: 10.3389/fenrg.2023.1291552

A novel distributing–collecting on-line insulation monitoring system and line selection technology for the DC supply system

Chen Feng, Pingfeng Ye, Zhengzhong Gao*, Haiyang Jiang, Xiangyu Zang and Xiangxing Zhang

College of Electrical Engineering and Automation, Shandong University of Science and Technology, Qingdao, China

At present, the power supply system of 5G base stations is a micro smart grid, it generally uses 240 V DC power supply with multiple branches, and leakage accidents will threaten personal and property safety, so it is vital to identify the fault line accurately and remove the faults rapidly. In this paper, the leakage phenomenon of transmission lines in the HVDC power supply system of a 5G communication base station is studied. To address the issue of multi-branch line leakage diagnosis and line selection in the 240 V DC system, a new distributed DC insulation monitoring and fault line selection technology and system are proposed. The distributed DC insulation monitoring line selection technology is used to collect the leakage current of each branch by setting a unique single-core DC leakage transformer and process the signal primarily. In addition, a high-resistance bridge switchgear is added to the bus bar. According to different leakage currents caused by the imbalance of the bridge before and after the switch, the insulation resistance of electrodes to the ground is calculated accurately, which solves the problem that the current technology cannot judge the fault of the positive and negative electrodes to the ground at the same time. Through both simulation and prototype experiments, the feasibility of this technology and system device in line insulation monitoring and line selection of the HVDC communication base station power supply system is verified.

KEYWORDS

insulation monitoring system, leakage phenomenon, fault line selection, grounding selection for DC system, simulation and prototype experiments

1 Introduction

Currently, a high-voltage DC power supply system with a voltage level of 240 V is widely used as equipment in a signal system, transformer substation, and communication station because of the complicated environment (Hellgren, 2004; Li, 2012; Chen, 2018a). As these DC power supply systems include many branches and loads, when the line insulation drops, it is easy to cause grounding, short circuit, and other faults, endangering personal safety or equipment safety. Therefore, it is necessary to have a corresponding insulation monitoring device, which can give early warning and lock the fault location quickly.

At present, the integral insulation monitoring and protection technology is adopted in the power supply of communication station usually. However, it is impossible to select and locate the faulty branch accurately. The existing insulation monitoring methods with the function of fault branch selection include the balance-bridge method and signal injection method. However, there are also many problems in these methods. For the balance-bridge method of fault line selection, it is necessary to set the bridge's parameters accurately, according to the system type (Huang et al., 2019). If the value of the bridge parameter is low, the insensitivity of the insulation monitoring system will cause an inaccuracy of the fault judgment. On the contrary, if the value of the bridge parameter is high, the test data will have large deviation and the equipment maintenance cost will increase. Furthermore, it is difficult to detect the simultaneous decline of positive and negative insulation resistances to the ground with current technology (Luo et al., 2016). In order to detect the insulation state of each electrode, switchable bridges need to be installed in each branch. This bridge has caused the line-to-ground insulation resistance to drop actually. For each additional bridge, the equivalent value of the ground resistance will be doubled, and the risk of personal electric shock will increase accordingly (Jiang and Ji, 2009; Yin et al., 2012; Rybski et al., 2015). At the same time, on one hand, the active power leakage current sensor installed in the branch is costly; on the other hand, it is ineffective to detect all kinds of insulation faults. The signal injection method is greatly affected by the electrical distribution parameters, and it is impossible to judge the insulation drop in the complicated environment (Yow-Chyi and Chen-You, 2012; Olszowiec, 2017).

To solve these issues, a distributing–collecting online insulation monitoring system is proposed. It adopts the single-core DC-type current transformers settled in each branch to collect the micro-current after the insulation fault. Ground insulation monitoring and line selection can also be realized under various insulation faults. This paper mainly includes the following aspects: the principle and technology of leakage protection are analyzed, and the sensor suitable for the distributed acquisition system is studied. The advantages and disadvantages of current leakage protection technology are compared and analyzed. A novel distributing–collecting on-line insulation monitoring system is proposed, which is more suitable for the DC transmission system of communication base stations and the use of remote electrical equipment. The hardware structure and algorithm principle of the proposed system are developed and designed. It is best to build the analog communication base station of the DC transmission system using MATLAB software verification and prototype verification, carry out experimental verification, and analyze the results to verify the effectiveness of the system device.

2 Method

2.1 Personal electrical safety issues and insulation monitoring settings

With reference to the provisions of China's electrical safety regulations (GB/T 13870.2-2016), the human body safety current in the DC system is no more than 50 mA, i.e., when the current flowing through the human body is below 50 mA, it is not life-threatening, and people who are subjected to an electric shock can react in time and avoid continuous injury (Dawalibi et al., 1990). For the DC power supply system, it is stipulated that the product of the human electric shock current and the action time is not more than 30 mA s. By imitating the safety parameters of the AC system, the safety parameter for the DC system can be stipulated as 50 mA s. According to China's human body safety current standard, adult men's threshold to get rid of the electric shock should be no more than 10 mA (Roberts, 2009; Zhao et al., 2017; Zhenbin et al., 2021).

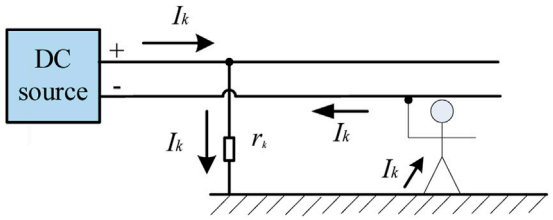

FIGURE 1
DC personal electric shock safety diagram.

As shown in Figure 1, the line in the figure represents the line of the general DC power supply system. When a person touches the positive pole or negative pole of the line and the insulation of the other pole drops, an electric shock accident will occur.

Generally, the resistance of the human body r_{bady} is regarded as 1 kΩ, and the voltage level of the DC power supply system for the communication system is 240 V.

$$I_k = \frac{U_0}{r_k + r_{\text{bady}}}. \tag{1}$$

Calculated by Eq. 1, when the insulation resistance r_k of the line (positive or negative pole) drops to 3.8 kΩ, if the person happens to touch the other pole (negative or positive pole) of the line, the current flowing through the person is 50 mA (human body safety current for the DC system). When the insulation resistance of the line drops to 24 kΩ, the current flowing through the body is 9.6 mA (the threshold current to get rid of the electric shock).

In order to guarantee the human safety and ensure certain reliability, the current flowing through a person must be controlled under 50 mA. Since the communication system powered by the DC power supply system is generally installed in a high tower, there is a great danger of muscle suppression caused by an electric shock. Therefore, for avoiding an electric shock and enabling people to get rid of the electric shock in time, it is recommended to set the tripping operation setting as 28 kΩ (1.2 times of 24 kΩ).

2.2 Distributed online insulation monitoring system

2.2.1 The structure of a distributed online insulation monitoring system

Aiming at the deficiency of the existing insulation monitoring system, this paper proposes a distributed online insulation monitoring

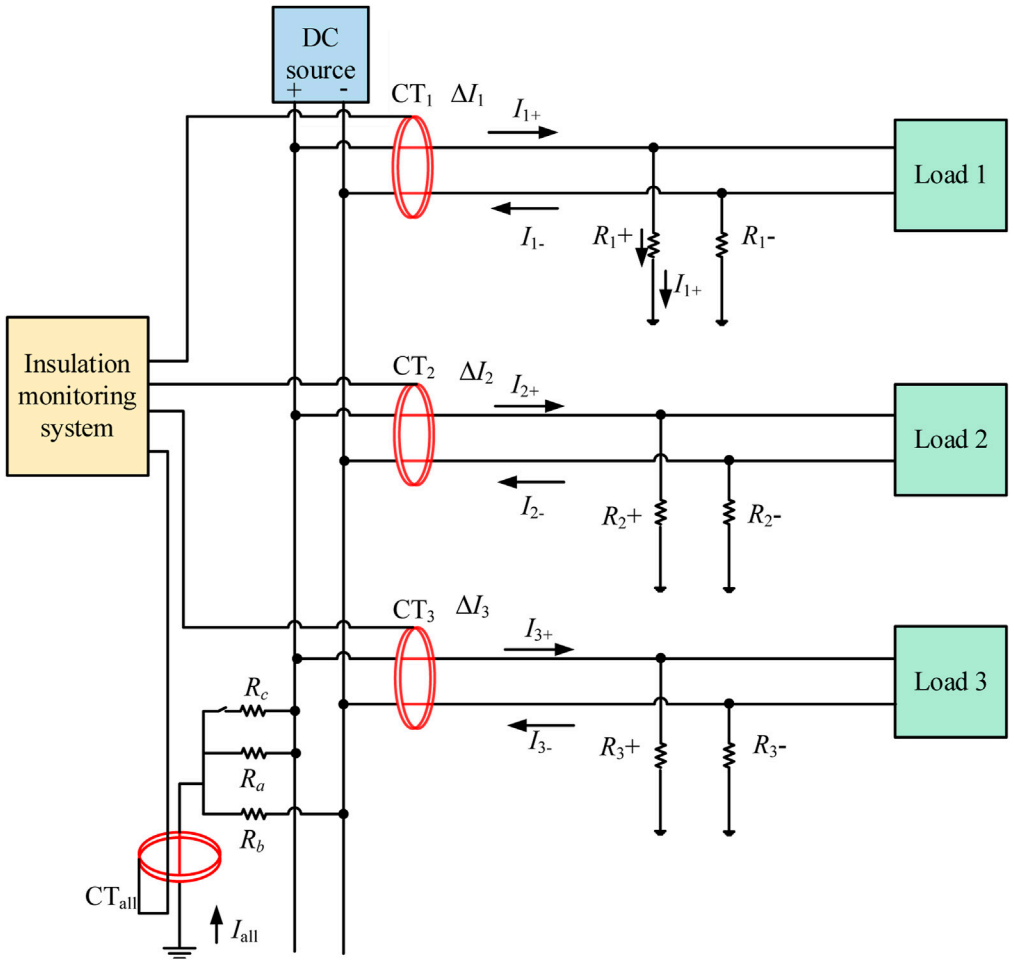

FIGURE 2
Distributed online insulation monitoring system.

system. Figure 2 displays the distributed insulation monitoring system. The whole system consists of a centralized central processing unit and a dedicated DC residual current transformer distributed in each branch. Positive and negative cable currents in each branch pass through the special DC residual current transformer proposed in this paper at the same time, and the residual current of each branch is extracted using the principle of the current magnetic field effect canceling each other in the positive and negative cables for insulation monitoring. All control signal transmission, signal collection, and processing are integrated in the central processing unit of the distributed insulation monitoring device. The central processing unit uniformly sends out the control signal, controls, and modulates the special DC transformer to collect the signal, and the collected signal is uniformly processed by the central processing unit. CT_1, CT_2, … CT_n are DC insulation monitoring transformers installed in each branch, and CT_{all} is the DC insulation monitoring transformer, which is installed at the bus with a high resistance to ground. R_{1+}, R_{1-}, R_{2+}, R_{2-} … R_{n+}, and R_{n-} are the insulation resistances of each branch. R_a and R_b are the balanced high resistance to the ground of the bus.

The entire system consists of a central processing unit and DC residual current transformers distributed over the branches. The transformer collects residual current of each branch for insulation monitoring by the principle that the magnetic field created by current in different directions cancels each other out.

2.2.2 Distributed online insulation monitoring transformer

By studying the existing magnetic modulation current transformers, a new insulation monitoring transformer is presented, which is more durable, precise, economical, and practical. The existing magnetic modulation current transformers are all active transformers; they usually require a control circuit, and a signal processing and amplifying circuit in them. An alternating current signal is added to the magnetic core, so the direct current of the DC power system can be extracted on the secondary side of the transformer. The current transformer is shown in Figure 3 (Chen and Sun, 2018; Xie et al., 2016; M; Shi et al., 2022).

The principle of the transformer is as follows: first, the central processing unit sends out the AC control signal, which is injected into the magnetic ring of the transformer. The acquisition coil transmits the collected signal back to the signal processing module of the central processing unit. Through signal processing, the DC component is extracted (Wang et al., 2020; Li et al., 2015). As shown in Figure 3, when the AC signal is injected into the injection

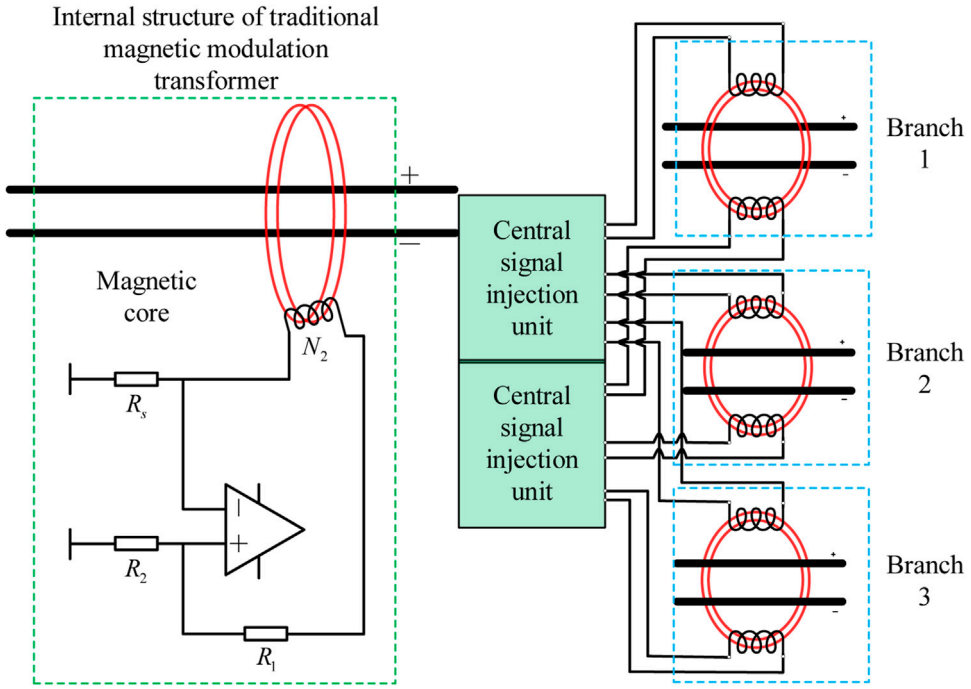

FIGURE 3
Traditional magnetic modulation and improved distributed modulation transformers.

coil on the magnetic ring in the transformer, the AC signal generates an alternating magnetic field in the magnetic ring. The line under test passes through the center of the magnetic core. If the line under test contains a DC signal, the DC signal will generate a magnetic field offset in a fixed direction in the magnetic ring. The acquisition coil collects the signals generated by the combined action of AC and DC signals on the magnetic field, and the injected magnetic field is changed by the bias of the DC magnetic field (Zhao et al., 2012; Chen et al., 2019). The collected signal is processed to obtain the DC current of the line under test. In order to further reduce the cost, the central processing unit of the insulation monitoring system is proposed to inject ac control signals into the transformers of each branch, control the magnetic-modulated current transformer to extract the dc current, and collect the residual current of each branch by the central processing unit so as to judge the insulation decline state. This method does not require the transformer of each branch to install the control circuit, and signal processing and amplification circuit separately and greatly reduces the cost of the transformer; the control signal is uniformly sent by the central processing unit, reducing the error and improving the reliability of insulation monitoring.

The development board of arm STM32F103 selected in this paper is equipped with three 12-bit ADC converters, with an AD sampling rate up to 1 MHz. Because the ADC converter can only collect 0–3.3 V voltage signal and the transformer secondary side current signal is given, we need to regulate the transformer secondary side of current signal, as shown in Figure 4. After current voltage conversion, the in-phase amplifier, pressure limiting protection, signal processing steps, such as isolation, and low pass filtering can be collected to the transformer secondary side current signal, to arm for analysis and calculation.

2.2.3 Analysis and determination for the insulation fault

In view of the possibility of each cable in the complex DC power system having an insulation drop, the distributed insulation monitoring system can realize the real-time online monitoring of the insulation state of each branch in the system.

Figure 2 shows high-resistance grounding in the DC power supply system. If the grounding fault or insulation degradation occurs in the positive pole of branch 1, there is leakage current I_{1+}, which flows into the earth and flows back to the negative pole through high-resistance grounding of the bus; at this time, the current of branch 1 is increased and $\Delta I_1 > 0$. Transformer 1 of branch 1 can collect the DC leakage current in real-time and upload it to the central processing unit.

Figure 2 shows R_a and R_b are the high resistance of neutral point grounding bus, communication equipment in the 240V power supply system. The resistance value is generally set to 200 kΩ. R_{n+} and R_{n-} are the positive and negative insulation resistance of the n branch. The cable-related parameters show the system of intact cable insulation resistance of approximately 40 MΩ. Taking branch n as an example, Figure 5 shows the simplified circuit. R_a, R_b, R_{n+}, and R_{n-} constitute the bridge balance. When no insulation drop occurs, R_{n+} is equal to R_{n-}, R_a is equal to R_b, and the bridge becomes balanced, and $\Delta I_n = I_{n+} - I_{n-} = 0$.

When a single-terminal ground fault occurs, the positive insulation resistance R_{n+} in branch n decreases, the negative resistance R_{n-} remains unchanged, and the bridge is unbalanced. The leakage current flows from the positive electrode through the positive insulation resistance R_{n+} into the earth and flows back to the negative electrode from the bus high resistance R_b to form a circuit. At this point, the measured current of the branch n CT_n is

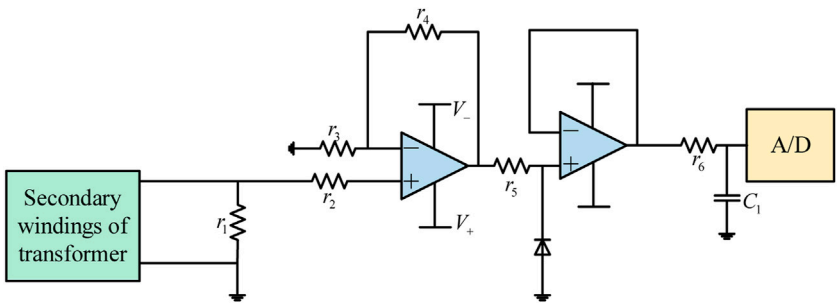

FIGURE 4
Signal conditioning circuit.

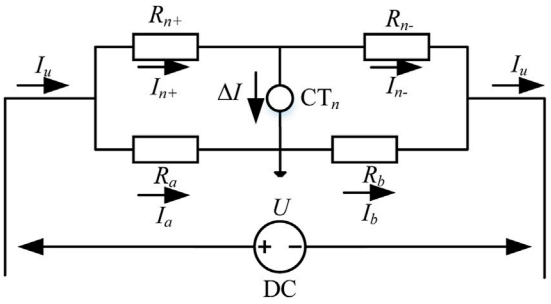

FIGURE 5
Equivalent circuit of the single-pole grounding fault.

$\Delta I_n = I_{n+} - I_{n-} \neq 0$. Since the negative resistance R_{n-} is unchanged, $I_{n-} \approx 0$; it is negligible, so $\Delta I_n = I_{n+}$.

According to the Kirchhoff's voltage law (Quintela et al., 2009),

$$U = R_a I_a + R_b (\Delta I_n + I_a), \tag{2}$$

$$R_{n+} = \frac{R_a I_a}{I_{n+}} = \frac{R_a [U - R_b \Delta I_n]}{I_{n+}}. \tag{3}$$

Because the anode voltage U is observed to be 240 V, high-resistance R_a and R_b are 200 kΩ; the drain-current value ΔI_n is obtained from the transformer CTn, and the value of positive insulation resistance R_{n+} can be obtained.

Similarly, if the negative monopole insulation drops, the negative insulation resistance R_{n-} in the branch n drops, the positive resistance R_{n+} remains unchanged, the bridge is unbalanced, and the leakage current flows from the negative electrode through the negative insulation resistance R_{n-} into the earth and flows from the bus high-resistance R_a back to the positive electrode to form a circuit, which is opposite to the positive insulation decreasing leakage current. At this point, the current measured by CTn in branch n is $\Delta I_n^{'}$. $\Delta I_n^{'} = I_{n+} - I_{n-} \neq 0$. Since the positive resistor R_{n+} is unchanged, $I_{n+} \approx 0$; it is negligible, so $\Delta I_n^{'} = I_{n-}$.

$$U = R_b I_b + R_a \left(\Delta I_n^{'} + I_b\right), \tag{4}$$

$$R_{n-} = \frac{R_b I_b}{I_{n-}} = \frac{R_b [U - R_a \Delta I']}{\Delta I_n^{'} (R_a + R_b)}. \tag{5}$$

Because the anode voltage U is considered to be 240V, high-resistance R_a and R_b are obtained to be 200 kΩ, the leakage current value ΔI_n is obtained by CT$_n$, by substituting Eq. 5, and the value of negative insulation resistance R_{n-} can be obtained.

Section 2.1 has been demonstrated that the insulation resistance alarm value should be greater than 28 k.

Therefore, the set values for the insulation monitoring system are $R_n \geq 2.8 \times 10^4 \Omega$. It can be found that the positive electrode-to-earth insulation fault and the negative electrode-to-earth insulation fault measure the opposite current direction when the monopole insulation fault occurs. Then, the calculation shows that the insulation resistance is less than the setting value when $|\Delta I_n| \leq 5.26 \times 10^{-4}$A. Therefore, when the system branch transformer detects leakage current $|\Delta I_n| > 5.26 \times 10^{-4}$A, the system raises an alarm and through ΔI_n direction to determine the positive or negative insulation fault.

The monitoring principle analysis and formula derivation for the single-terminal grounding fault are mentioned previously. This principle can also be extended to realize the on-line monitoring function for insulation of one or more branches at the same time. It is only necessary to calculate the insulation resistance of each branch individually.

However, in the DC power supply system, in addition to the monopole insulation drop, there are also single-branch double-stage insulation drop faults. Because the aforementioned principles are derived from the monopole insulation drop, it is not applicable to the case of the anode and cathode simultaneous drop. Therefore, the balanced resistance switching principle is adopted in this paper, that is, a resistance switching device is added to the high-resistance connection of the distribution bus to realize the monitoring technology of this kind of fault. Figure 6 shows that a new resistance R_c and switching device are added to the positive pole of the bus. The switching device is selected to be closed every 5 s for a duration of 1 minute before disconnecting. Its simplified equivalent circuit diagram is shown in Figure 6.

In Figure 6, the initial state of switch K is state 1. R_a and R_b are the high resistances at the neutral point of the bus; R_c is the switchable high resistance, which is used to change the state of the bridge; R_{n+} and R_{n-} are, respectively, the insulation resistance values of positive and negative pole cables in branch n; and ΔI_n is the leakage current, $\Delta I_n = I_{n+} - I_{n-}$. U_2 is the negative electrode-to-earth voltage, which is the terminal voltage of R_b or R_{n-}.

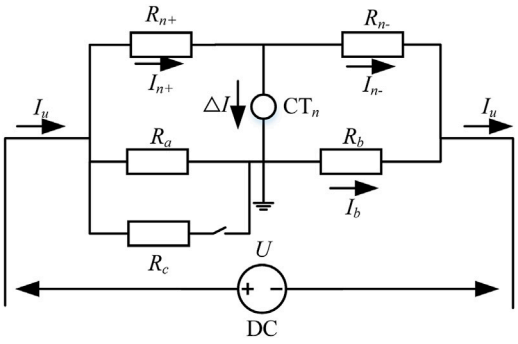

FIGURE 6
Equivalent circuit diagram.

If the positive and negative pole wires of branch n suffer from insulation decline at the same time, the equation under state 1 can be obtained according to the following circuit principle:

$$\frac{U}{R_a//R_{n+} + R_b//R_{n-}} = \frac{U_2}{R_b//R_{n-}}, \tag{6}$$

$$U_2 = (I_a + \Delta I_n)R_b, \tag{7}$$

$$U_2 = U - I_a R_a. \tag{8}$$

Combining Eqs 7, 8, we observe that

$$I_a = \frac{U - \Delta I_n R_b}{R_a + R_b}, \tag{9}$$

$$U_2 = \frac{R_b(U + \Delta I_n R_b)}{R_a + R_b}. \tag{10}$$

Switch K is closed, followed by state 2; $\Delta I_n^{'}$ is the leakage current at state 2, where $\Delta I_n^{'} = I_{n+}^{'} - I_{n-}^{'}$. $U_2^{'}$ is the negative electrode-to-earth voltage, that is, the terminal voltage of R_b or R_{n-} can be obtained according to the following circuit principle:

$$\frac{U}{R_a//R_c//R_{n+} + R_b//R_{n-}} = \frac{U_2^{'}}{R_b//R_{n-}}, \tag{11}$$

$$U_2 = \left(I_a^{'} + \Delta I_n^{'}\right)R_b, \tag{12}$$

$$U_2^{'} = U - I_a^{'} R_a. \tag{13}$$

Combining Eqs 12, 13, we observe that

$$I_{ac} = \frac{U - \Delta I_n^{'} R_b}{R_a//R_c + R_b}, \tag{14}$$

$$U_2^{'} = \frac{R_b\left(U + \Delta I_n^{'} R_b\right)}{R_a//R_c + R_b}. \tag{15}$$

Combining Eqs 6, 11, we observe that

$$R_{n+} = \frac{1}{\frac{R_a//R_c}{R_a R_b} \times \frac{\left(U - \Delta I_n^{'} R_b\right)(R_a + R_b)}{\left(U + \Delta I_n^{'} \times R_a//R_c\right)(R_a + R_b) - (U + \Delta I_n R_a)\left(R_a//R_c + R_b\right)}}, \tag{16}$$

$$R_{n-} = \frac{1}{\frac{R_a^2(R_a + R_b)}{R_b^2(U + \Delta I_n R_a)(R_a + R_b)} \times \frac{(U - \Delta I_n R_b)\left(U - \Delta I_n^{'} R_b\right)}{\left(U + \Delta I_n^{'} \times R_a//R_c\right)(R_a + R_b) - (U + \Delta I_n R_a)\left(R_a//R_c + R_b\right)}}. \tag{17}$$

Because R_a, R_b, and R_c are known for 200 kΩ, U is the negative voltage on both ends as its value is 240 V, and $\Delta I_n^{'}$ and ΔI_n can be measured using a branch transformer, which can calculate the value of insulation resistance R.

Therefore, when the transformer of the branch and the transformer of the high-resistance side of the bus bar detect leakage current, the decrease in the conductor insulation resistance value can be determined in real time, according to the direction and size of the leakage current of the positive and negative branches. If the value is less than the setting value, the system will give an alarm and produce corresponding actions. Compared to the probability that both poles of a branch have an insulation decrease, a single-pole insulation fault is more likely to happen. So, it is necessary to allocate time for monitoring each fault in a reasonable way. Table 1 shows the time allocation for switch K switching to monitor two faults. The resistance switching device is the switch K shown in Figure 2.

The switching frequency of switch K is 6 s/time. If switch K is closed, the bridge is unbalanced, and the system is efficient to detect the condition that the insulation resistance of the positive and negative poles is decreased to the same value at the same time. Furthermore, if the switch is turned off, a single-pole insulation decrease could be detected in this mode.

3 Results

3.1 Simulation of the single-electrode grounding fault

The Simulink model based on MATLAB is shown in Figure 7.

First, the state of the power supply system during normal operation is simulated and analyzed. When the insulation is well, the insulation resistance of each branch is approximately 40 MΩ. The results show that the leakage current measured by each transformer is 0.

The second step is to simulate monopole to ground insulation descent. Branch 1 is set as the faulty branch. In order to ensure the diversity and comprehensiveness of the simulation, it is assumed that the grounding resistance of the branch with an insulation fault is 100 kΩ, 75 kΩ, 50 kΩ, 28 kΩ, and 8 kΩ. When the monopole insulation drops in the positive or negative insulation, the leakage current value is equal, and the current direction is opposite. It can be determined whether the positive insulation or the negative insulation decreases by the current direction. Therefore, only the positive insulation decreases are simulated.

As shown in Figure 8, the comparison between the simulation results and the calculation formula shows the relationship between the leakage current and insulation resistance when different monopole-to-ground insulation resistance values are simulated. The curve in the figure is the formula of calculating insulation resistance by leakage current in Section 2 of this paper.

When the monopole-to-the ground insulation fault occurs, the smaller the monopole-to-the ground insulation resistance is, the greater the leakage current will be. The simulation results are in perfect agreement with the calculated results. Through comparison, it can be seen that the formula proposed in this paper can accurately

10.3389/fenrg.2023.1291552

TABLE 1 Time allocation of switch K.

Condition of K	Switching cycle of K (s)	Monitoring mode
Closed	1	Balanced insulation decreases in two poles of the branch
Broken	5	Single-pole insulation decreases

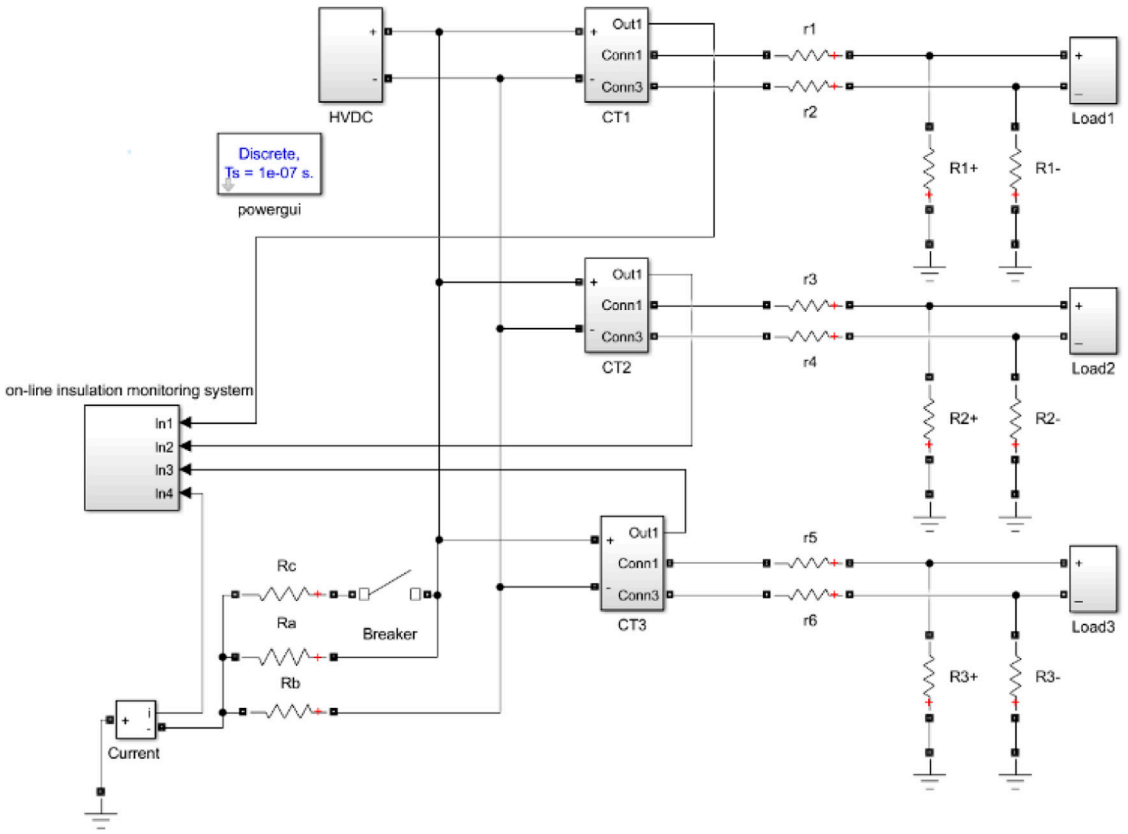

FIGURE 7
Simulation mode of the distributed insulation monitoring system.

calculate the insulation resistance for the monopole insulation decline.

If there is insulation degradation in multiple branches at the same time, there will be leakage current in all branches with an insulation fault and the high-resistance grounding bus-bar. Therefore, it could recognize insulation degradation in all branches through this technology.

3.2 Simulation of the multi-electrode grounding fault

In the third step, the insulation of the anode and cathode drops at the same time. In the simulation figure, the branch containing Rc contains a circuit breaker to simulate the two states of bridge resistance before and after switching (before the cut is state 1 and after the cut is state 2). In order to carry out a comprehensive analysis, the following positive and negative insulation resistance values are selected: 150 kΩ, 100 kΩ, 75 kΩ, 50 kΩ, 28 kΩ, and 8 kΩ. Leakage current ΔI under state 1 and leakage current $\Delta I'$ under state 2 were measured, and the data were drawn in the three-dimensional coordinate system, as shown in red dots in Figures 9, 10, respectively, for the simulation results. In the figure, x axis and y axis represent positive and negative insulation resistance, respectively. The z-axis in the two figures shows the leakage current ΔI under state 1 and the leakage current $\Delta I'$ under state 2. Eqs 18, 19 were recorded into the coordinate system, as shown in the surface in Figure 9. When the positive and negative insulation resistances were given different values, the leakage current ΔI under state 1 and the leakage current $\Delta I'$ under state 2 were shown.

In state 1, the greater the difference between the positive electrode-to-ground insulation resistance and the negative electrode-to-ground insulation resistance is, the greater the

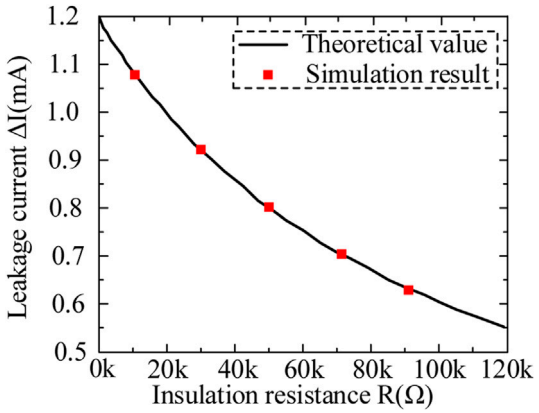

FIGURE 8
Simulation results and the calculation formula.

leakage current value will be, and the direction is related to the insulation resistance at the poles. When $R_{n+} > R_{n-}$, the leakage current is negative; when $R_{n+} < R_{n-}$, the leakage current is positive; and when $R_{n+} = R_{n-}$, the leakage current is 0. At this point, it is impossible to judge the insulation resistance to the ground, so the bridge resistance needs to be switched to state 2. In state 2, it can be seen that due to the imbalance of high resistance of bus grounding, when the positive electrode-to-earth insulation resistance is much greater than the negative electrode-to-earth insulation resistance, the leakage current value is the maximum, and the leakage current is negative. When $R_{n+} \times R_b = R_{n-} \times R_{a//c}$, the leakage current is 0 due to the bridge balance.

It can be seen from the comparison that the formula proposed in this paper can accurately calculate the insulation resistance of the anode and cathode for the simultaneous decline of the anode and cathode insulation.

3.3 Analysis of the experiment

In order to test the proposed distributed insulation monitoring system in this paper, an experimental setup was built, and a prototype device of the system was made for experiments. Figures 11 and 12 shows the experimental setup of insulation monitoring system proposed in this paper. Eight branches can be collected and calculated simultaneously. Figure 11 shows the central processing module of the system in this paper, whose function is to transmit the detection control signal, process the collected signal, calculate the insulation resistance, and complete the alarm or transmit the result to the upper computer. As shown in Figure 12, the signal acquisition module passes the positive and negative poles of each branch through the center of the current transformer at the same time.

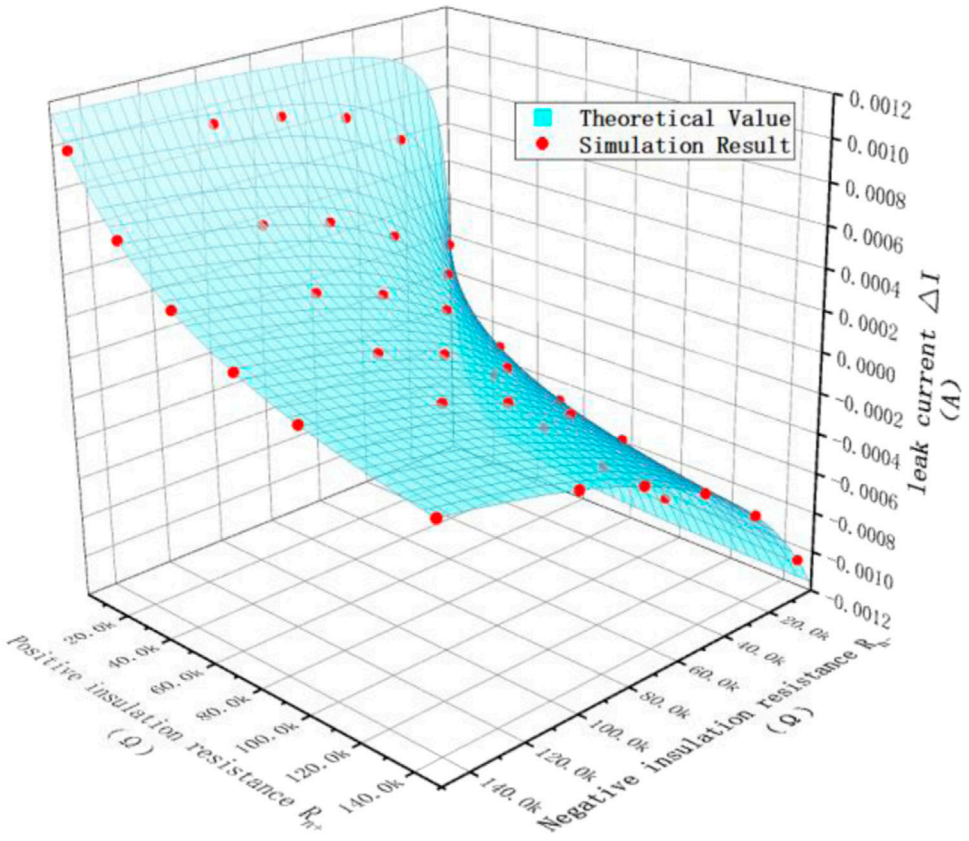

FIGURE 9
Simulation results are compared with the theoretical values under state 1.

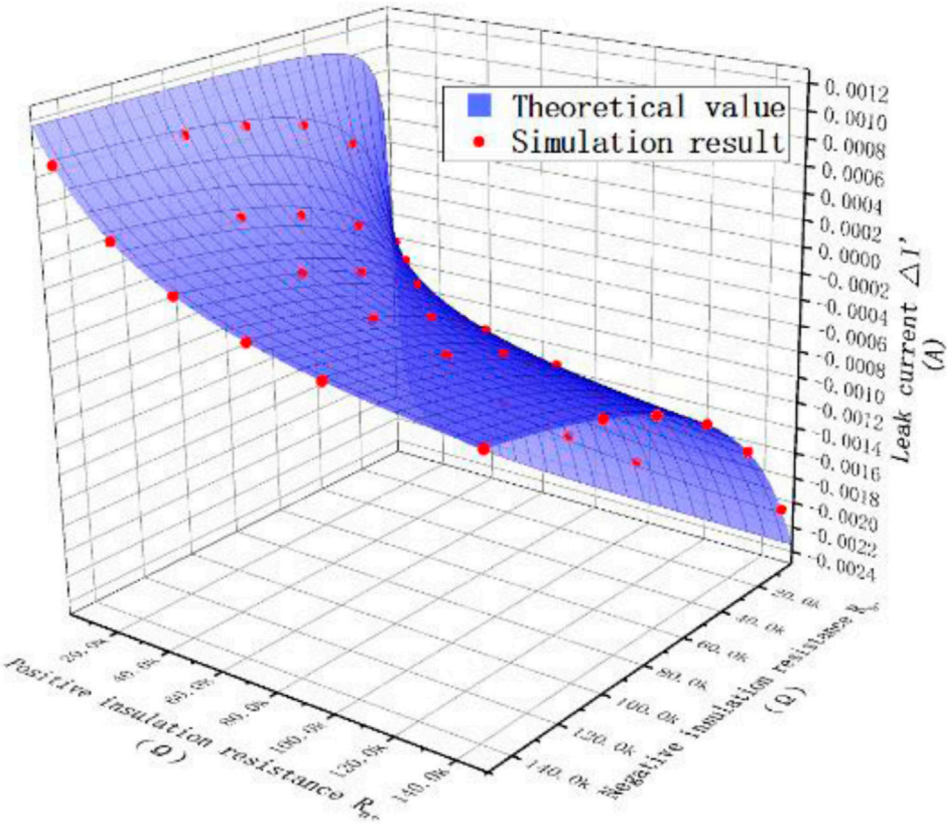

FIGURE 10
Simulation results are compared with the theoretical values under state 2.

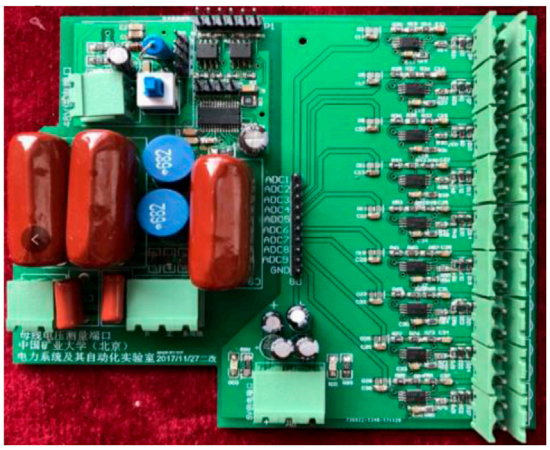

FIGURE 11
Central processing module of the system.

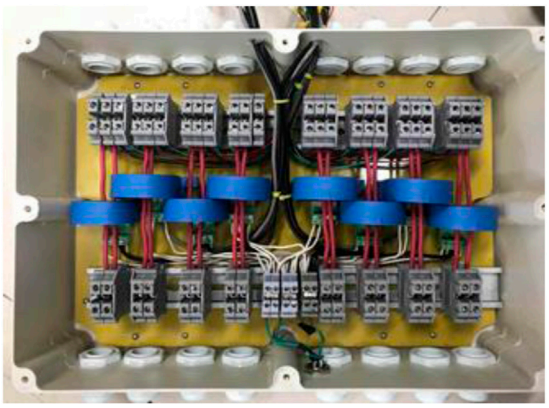

FIGURE 12
Transformer connection situation.

The current transformer sends the acquisition signal to the A/D acquisition module of the central processing module and to the oscilloscope used in the experiment. The positive and negative lines of one branch are simultaneously passed through the single-core DC current transformer. The transformer is powered by the central processing module, and the range is ± 10uA~2 mA. The circuit of the transformer is shown in Figure 13.

First, the single insulation drop detection was verified. In order to carry out a comprehensive analysis, three branches were selected for the failure test. For each branch, first, the negative insulation resistance was kept unchanged, and the positive electrode was

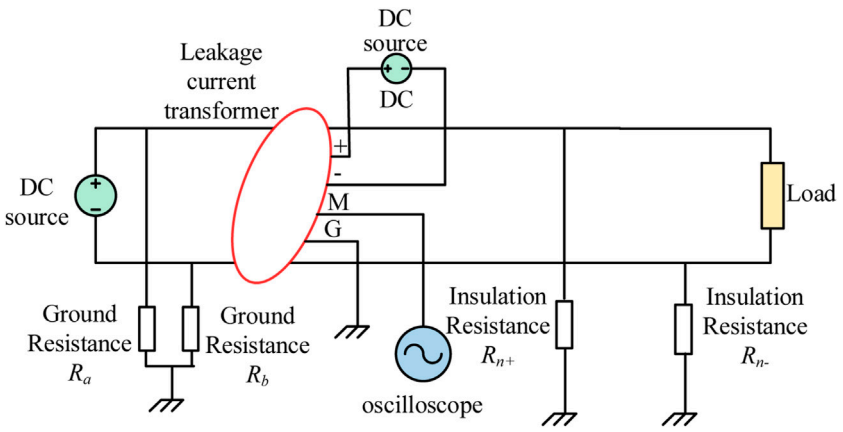

FIGURE 13
Experimental equivalent circuit.

TABLE 2 Simulation and theoretical parameter table of multi-branch cable insulation monitoring.

Positive insulation resistance/KΩ	Negative insulation resistance/KΩ	State 1 leakage current ΔI/mA	State 2 leakage current ΔI′/mA	Calculated value of positive insulation resistance/KΩ	Calculated value of negative insulation resistance/KΩ	Positive insulation resistance error rate	Negative insulation resistance error rate
150	150	0	−0.280	153	151	2%	0.66%
150	28	−0.662	−1.331	150.2	28	0.1%	0%
100	28	−0.539	−1.232	100.2	28.2	0.2%	0.7%
100	75	−1.116	−0.522	101	75.8	1%	1.06%
75	50	−0.120	−0.062	76.5	51	2%	2%
75	28	−1.674	−1.12	75.4	28.3	0.5%	1%
50	50	0	−0.436	51	51	2%	2%
28	50	0.288	−0.071	27.3	48.7	−2.5%	−2.6%
28	8	−0.631	−1.46	28.3	8.08	1%	1%
8	28	0.627	−0.36	27.8	7.99	0.71%	1.25%

connected to the ground, 100 kΩ, 75 kΩ, 50 kΩ, 28 kΩ, and 8 kΩ. Multiple measurements of leakage current ΔI are averaged. Figure 14 shows the comparison between the experimental results and theoretical calculations. The error bar represents experimental data, and the curves are theoretical values. It is observed that the lower the insulation resistance to ground is, the smaller the resulting error will be.

It can be seen from this that the designed prototype can accurately determine and calculate the single pole-to-ground insulation resistance drop fault.

Then, the condition of positive and negative insulation resistances falling simultaneously was verified, the system bus contained switching resistance R_c, the resistance value of positive and negative insulation resistances to the ground was changed, and the leakage current ΔI before switching and $\Delta I'$ after switching was recorded. As shown in the following table, the calculated insulation parameter and its error for system with multi-branch insulation degradation are shown in Table 2.

The comparison between the calculated insulation parameters and the theoretical insulation parameters shows that the monitoring error of the system will gradually increase with the decrease in the difference of positive and negative line insulation resistances. However, the error of insulation resistance calculated by the system based on distributed selection is less than ± 3%, which fully meets the basic requirements of the system. Therefore, this principle can be applied to online insulation monitoring for all kinds of degradation.

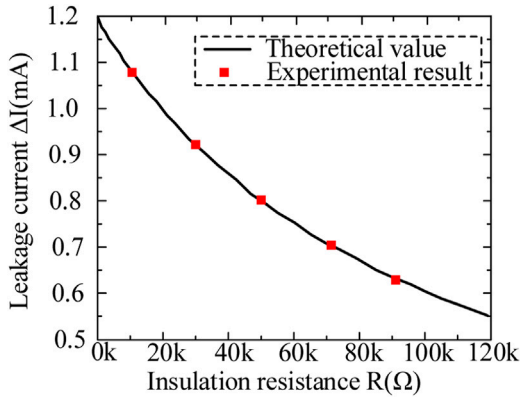

FIGURE 14
Comparison experimental results and theoretical calculation of the single branch.

4 Conclusion

Based on the analysis of the existing problems of the leakage protection technology for DC power supply systems in domestic and abroad, and focus on the insulation degradation fault of the DC power system in the communication station, this paper proposes an on-line insulation monitoring system based on distributed selection. This system can realize online insulation monitoring, and can quickly and accurately diagnose the faulty branch with insulation degradation, single-line grounding fault, and the grounding fault of the remote equipment shell

Through experiments and simulations, the conclusions are as follows:

(1) When the monopole-to-ground insulation drops, the smaller the monopole-to-ground insulation resistance is, the greater the leakage current will be. The simulation and experiment basically agree with the calculation results, which prove that the formula proposed in this paper can calculate the insulation resistance accurately.
(2) When both positive and negative insulation resistances are decreased, in state 1, the larger the difference between the positive pole-to-ground insulation resistance and the negative pole-to-ground insulation resistance is, the larger the leakage current value will be, and the direction is related to the insulation resistance at the poles. When $R_{n+} > R_{n-}$, the leakage current is negative; when $R_{n+} < R_{n-}$, the leakage current is positive; and when $R_{n+} = R_{n-}$, the leakage current is 0. At this point, it is impossible to judge the insulation resistance to the ground, so the bridge resistance needs to be switched to state 2. In state 2, it can be seen that due to the imbalance of high resistance of bus grounding, when the positive electrode-to-earth insulation resistance is much greater than the negative electrode-to-earth insulation resistance, the leakage current value is the maximum, and the leakage current is negative. When $R_{n+} \times R_b = R_{n-} \times R_{a//c}$, the leakage current is 0 because of the bridge balance. The simulation results are in good agreement with the calculated values, which proves the theory proposed in this paper. Compared with the calculated results, the experimental results have some errors; the error rate is less than 3%, in line with the general engineering standards. Therefore, it is shown that the distributed DC insulation on-line monitoring technology proposed in this paper can accurately complete the calculation and fault judgment of the positive and negative insulation resistances of each branch.

Data availability statement

The original contributions presented in the study are included in the article/Supplementary Material; further inquiries can be directed to the corresponding author.

Author contributions

CF: methodology and writing—original manuscript. PY: data curation, and writing—review and editing. ZG: resources, supervision, and writing—review and editing. HJ: formal analysis, and writing—review and editing. XZa: investigation, and writing—review and editing. XZh: writing—review and editing.

Funding

The authors declare that no financial support was received for the research, authorship, and/or publication of this article.

Conflict of interest

The authors declare that the research was conducted in the absence of any commercial or financial relationships that could be construed as a potential conflict of interest.

Publisher's note

References

Chen, Y. (2018a). Research on common DC current detection technolog. *Low. Volt. Appar.* 22, 82–86. doi:10.16628/j.cnki.2095-8188.2018.22.015

Chen, Y., and Sun, J. (2018). Research on residual current protection device with DC component detectio. *Electr. Energy Manag. Technol.* 14, 37–41. doi:10.16628/j.cnki.2095-8188.2018.14.007

Chen, Z., Li, H., Liu, L., Xiang, L., and Bai, B. (2019). DC bias treatment of hybrid type transformer based on magnetic flux modulation mechanism. *IEEE Trans. Magnetics* 55 (6), 1–4. doi:10.1109/tmag.2019.2903566

Dawalibi, F. P., Southey, R. D., and Baishiki, R. S. (1990). Validity of conventional approaches for calculating body currents resulting from electric shocks. *IEEE Trans. Power Deliv.* 5 (2), 613–626. doi:10.1109/61.53063

Hellgren, O. (2004). "A key to expanding older DC systems with new equipment," in *Intelec 2004. 26th annual international telecommunications Energy conference*, 241–247. doi:10.1109/INTLEC.2004.1401473

Huang, Y., Qin, J., Liu, N., Huang, H., Zhang, J., Bi, L., et al. (2019). Differential current method of unbalanced bridge with double bridge arm for DC insulation detection. *Electr. Energy Manag. Technol.* 11, 57–61. doi:10.16628/j.cnki.2095-8188.2019.11.011

Jiang, J., and Ji, H. (2009). "Study of insulation monitoring device for DC system based on four-switch combination," in *2009 international conference on computational intelligence and software engineering*, 1–4. doi:10.1109/CISE.2009.5363460

Li, H. (2012). Application analysis of high voltage DC power supply system (240V) in a test project. *Intelec* 2012, 1–7. doi:10.1109/INTLEC.2012.6374511

Li, K., Niu, F., Wu, Y., Wang, Y., Dai, Y., Wang, L., et al. (2015). Nonlinear current detection based on magnetic modulation technology. *IEEE Trans. Magnetics* 51 (11), 1–4. Art no. 4004804. doi:10.1109/tmag.2015.2446134

Luo, Z., Ren, X., Yang, H., Cai, G., Qing, C., and Luo, Y. (2016). "Research on the insulation monitoring devices for DC power system based on the detection technology of DC bus to grounding capacitance," in *2015 2nd international forum on electrical engineering and automation*, 117–120. doi:10.2991/ifeea-15.2016.24

Olszowiec, P. (2017). Influence of insulation monitoring devices on the operation of DC control circuits. *Power Technol. Engineeing* 6 (50), 653–656. doi:10.1007/s10749-017-0768-1

Quintela, F. R., Redondo, R. C., Melchor, N. R., and Redondo, M. (2009). A general approach to Kirchhoff's Laws. *IEEE Trans. Educ.* 52 (2), 273–278. doi:10.1109/te.2008.928189

Roberts, D. (2009). 50-V shock hazard threshold. *IEEE Trans. Industry Appl.* 46 (1), 102–107. doi:10.1109/TIA.2009.2036541

Rybski, R., Kaczmarek, J., and Kontorski, K. (2015). Impedance comparison using unbalanced bridge with digital sine wave voltage sources. *IEEE Trans. Instrum. Meas.* 64 (12), 3380–3386. doi:10.1109/TIM.2015.2444255

Shi, M., Miao, H., Fei, J., Ge, X., Xiao, X., Wu, F., et al. (2022). "The development of DC leakage current monitoring device," in *2022 IEEE 5th international electrical and Energy conference (CIEEC)* (Nangjing, China: IEEE).

Wang, S., Li, H., Liu, Q., Huang, Q., and Liu, Y. (2020). "Design of a DC residual current sensor based on the improved DC component method," in *2020 IEEE power & Energy society general meeting (PESGM)* (Canada: Montreal, QC), 1–5.

Xie, Z., Han, S., and Wang, L. (2016). "The magnetic modulation of DC transformer core characteristics analysis," in *2016 3rd international conference on information science and control engineering (ICISCE)*, 1433–1438. doi:10.1109/ICISCE.2016.306

Yin, G., Liu, Y., Xu, H., Li, M., and Li, J. (2012). "The new DC system insulation monitoring device based on phase differences of magnetic modulation," in *2012 international conference on systems and informatics (ICSAI2012)*, 585–658. doi:10.1109/ICSAI.2012.6223065

Yow-Chyi, L., and Chen-You, L. (2012). Insulation fault detection circuit for ungrounded DC power supply systems. *SENSORS* 2012, 1–4. doi:10.1109/ICSENS.2012.6411550

Zhao, H., Xiao, X., and Sun, Q. (2017). Identifying electric shock in the human body via α dispersion. *IEEE Trans. Power Deliv.* 33 (3), 1107–1114. doi:10.1109/TPWRD.2017.276616

Zhao, X., Li, L., Lu, J., Cheng, Z., and Lu, T. (2012). Characteristics analysis of the square laminated core under DC-biased magnetization by the fixed-point harmonic-balanced FEM. *IEEE Trans. magnetics* 48 (2), 747–750. doi:10.1109/tmag.2011.2174776

Zhenbin, C., Weiya, C., Xiangyu, C., Qiao, H., Lu, H., and Qiu, N. (2021). A new method of insulation detection on electric vehicles based on a variable forgetting factor recursive least squares algorithm. *IEEE Access* 9, 73590–73607. doi:10.1109/access.2021.3079332

10.3389/fenrg.2023.1291552

Nomenclature

Parameter

r_{bady}	Resistance of the human body
r_k	Insulation resistance
U_0	Voltage level of the DC power supply system for the communication system
CT_n	DC insulation monitoring transformers installed in branch n
CT_{all}	DC insulation monitoring transformer which is installed at the bus with high resistance to ground
R_{n+}/R_{n-}	Insulation resistance of branch n
R_a/R_b	Balanced high resistance to ground of the bus
U	Anode voltage
R_n	Set values for the insulation monitoring system
R_c	New resistance and switching device to the positive pole of the bus
K	Initial state of the switch

Variable

I_k	Current flowing through the body
I_{1+}	Leakage current
ΔI_n	Current increment of branch n
$\Delta I_n^{'}$	Current measured by CTn in branch n
U_2	Negative electrode-to-earth voltage
ΔI	Leakage current